

# Sensitivity of groundwater systems to CO<sub>2</sub>: Application of a site-specific analysis of carbonate monitoring parameters at the SACROC CO<sub>2</sub>-enhanced oil field

GCCC Digital Publication Series #12-01

K. D. Romanak  
R. C. Smyth  
C. Yang  
S. D. Hovorka  
M. Rearick  
J. Lu



**Keywords:**

Characterization; CO<sub>2</sub>-EOR (Enhanced oil recovery); Field study-SACROC-Scurry Co-TX; Modeling-Geochemical; Monitoring-groundwater-USDW

**Cited as:**

Romanak, K.D., Smyth, R.C., Yang, C., Hovorka, S.D., Rearick, M., and Lu, J., 2012, Sensitivity of groundwater systems to CO<sub>2</sub>: Application of a site-specific analysis of carbonate monitoring parameters at the SACROC CO<sub>2</sub>-enhanced oil field: International Journal of Greenhouse Gas Control, 6(2012): 142-152. GCCC Digital Publication Series #12-01.

Provided for non-commercial research and education use.  
Not for reproduction, distribution or commercial use.



(This is a sample cover image for this issue. The actual cover is not yet available at this time.)

**This article appeared in a journal published by Elsevier. The attached copy is furnished to the author for internal non-commercial research and education use, including for instruction at the authors institution and sharing with colleagues.**

**Other uses, including reproduction and distribution, or selling or licensing copies, or posting to personal, institutional or third party websites are prohibited.**

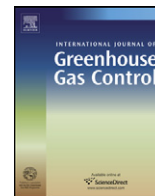
**In most cases authors are permitted to post their version of the article (e.g. in Word or Tex form) to their personal website or institutional repository. Authors requiring further information regarding Elsevier's archiving and manuscript policies are encouraged to visit:**

**<http://www.elsevier.com/copyright>**



Contents lists available at SciVerse ScienceDirect

## International Journal of Greenhouse Gas Control

journal homepage: [www.elsevier.com/locate/ijggc](http://www.elsevier.com/locate/ijggc)Sensitivity of groundwater systems to CO<sub>2</sub>: Application of a site-specific analysis of carbonate monitoring parameters at the SACROC CO<sub>2</sub>-enhanced oil fieldK.D. Romanak<sup>a,\*</sup>, R.C. Smyth<sup>a</sup>, C. Yang<sup>a</sup>, S.D. Hovorka<sup>a</sup>, M. Rearick<sup>b</sup>, J. Lu<sup>a</sup><sup>a</sup> Gulf Coast Carbon Center, Bureau of Economic Geology, Jackson School of Geosciences, The University of Texas at Austin, University Station, Box X, Austin, TX 78713, USA<sup>b</sup> Los Alamos National Laboratory, P.O. Box 1663, Los Alamos, NM 87545, USA

## ARTICLE INFO

## Article history:

Received 6 January 2011  
 Received in revised form  
 16 September 2011  
 Accepted 30 October 2011

## Keywords:

CO<sub>2</sub> sequestration  
 SACROC  
 Dedolomitization  
 Dockum  
 Carbon storage  
 Groundwater monitoring

## ABSTRACT

A field study and geochemical modeling of a shallow aquifer, situated above a long-running (>35 years), large-scale (~250 km<sup>2</sup>) CO<sub>2</sub>-enhanced oil recovery site (SACROC oil field), were conducted to determine how the aquifer might react to input of injectate CO<sub>2</sub>. Because calcite dissolution is widely accepted as the process that will result from CO<sub>2</sub> input into an aquifer, our assessment focused on carbonate-specific geochemical parameters (e.g., DIC, pH, Ca<sup>2+</sup>, and HCO<sub>3</sub><sup>-</sup>). After a careful characterization of the geochemical system of the Dockum aquifer above SACROC, a hypothetical leak of CO<sub>2</sub> was modeled into the system. Our analysis indicates that dedolomitization (dolomite dissolution with concurrent calcite precipitation) is the dominant native geochemical process and calcite dissolution cannot be assumed to result from CO<sub>2</sub> input. Dedolomitization, which is widely documented and common in many hydrologic systems, is driven in the Dockum above SACROC by both natural hydrologic and human-induced mechanisms. A sensitivity analysis under simulated CO<sub>2</sub> input for systems undergoing dedolomitization or calcite dissolution shows that both systems are relatively sensitive to CO<sub>2</sub>. Whereas the magnitude and direction of geochemical shift in pH, Ca<sup>2+</sup>, and HCO<sub>3</sub><sup>-</sup> depend on site-specific environmental factors, the shift in DIC is relatively similar in any of the modeled environments. The implication for monitoring geologic sequestration sites is that use of current monitoring parameters may require characterization of fundamental site-specific conditions for correct prediction of the consequences of CO<sub>2</sub> input; however characterization may not be necessary if DIC is used as the primary monitoring parameter.

© 2011 Elsevier Ltd. All rights reserved.

## 1. Introduction

## 1.1. Background

Monitoring of groundwater resources above geologic carbon sequestration reservoirs is proposed to ensure that potable water supplies remain protected and also to establish that CO<sub>2</sub> is adequately sequestered with respect to the biosphere (IPCC, 2005). As extensive application of geologic CO<sub>2</sub> sequestration is considered worldwide, determination of the potential for widespread usage of shallow aquifer geochemistry for CO<sub>2</sub> storage evaluation, as well as the parameters best-suited for monitoring these resources, is important.

In a hypothesized scenario of leakage from a CO<sub>2</sub> injection reservoir, CO<sub>2</sub> may rise buoyantly from the injection zone through breaches in sealing formations (i.e., faults) (Chang et al., 2009;

Zhang et al., 2009) or leaky plugged and abandoned wells (Gasda et al., 2009; Pan et al., 2009), or CO<sub>2</sub> may be carried upward in CO<sub>2</sub>-charged brine that is displaced by reservoir overpressuring (Bachu and Bennion, 2009; Nicot, 2008). In any case, CO<sub>2</sub> moving upward from a storage reservoir may eventually intersect and interact geochemically with fresh-water aquifers, rendering these environments fit for monitoring leakage.

The success of using shallow groundwater geochemistry as a tool for CO<sub>2</sub> storage evaluation depends on our ability to identify one or more geochemical parameters sensitive enough to provide a recognizable geochemical shift upon addition of exogenous CO<sub>2</sub> to the aquifer. This identification requires a shift that is larger than normal background variability and therefore detectable as an indicator of change. Widespread application of a standard method to a variety of geologic sequestration (GS) locations requires that the type and magnitude of geochemical shift are similar or at least predictable in any geochemical environment, even though hydrochemical processes and mineralogies differ widely among aquifers. In the absence of such a parameter, costly and time-consuming characterization of each aquifer above a carbon storage site is

\* Corresponding author. Tel.: +1 512 471 6136; fax: +1 512 471 0140.  
 E-mail address: [katherine.romanak@beg.utexas.edu](mailto:katherine.romanak@beg.utexas.edu) (K.D. Romanak).

needed to formulate effective site-specific geochemical monitoring plans.

The current position of many researchers is that the predictable consequence of CO<sub>2</sub> input into a dilute aquifer is calcite dissolution leading to (1) decrease in pH; (2) increase in dissolved inorganic carbon (DIC) as alkalinity or HCO<sub>3</sub><sup>-</sup>; (3) increase in Ca<sup>2+</sup> and/or Mg<sup>2+</sup> from dissolution of common carbonate minerals, calcite, and dolomite; and (4) eventual mobilization of metals from mineral dissolution and desorption reactions. Therefore, a popular suggestion is that carbonate parameters (pH, HCO<sub>3</sub><sup>-</sup> and Ca<sup>2+</sup>) may be suitable for relatively early detection of exogenous input of CO<sub>2</sub> into groundwater resources. Because carbonates are kinetically more favorable to reaction with CO<sub>2</sub> than silicates, geochemical shifts can result, even when silicates predominate volumetrically (Blum et al., 1998).

Hypotheses have emerged from studies that incorporate a broad number of approaches from theoretical modeling using compilations of aquifer databases (Apps et al., 2009; Carroll et al., 2009; Wang and Jaffe, 2004; Wilkin and DiGiulio, 2010; Zheng et al., 2009) to laboratory batch experiments (Lu et al., 2010; Yang et al., under revision), to controlled field experiments (Assayag et al., 2009; Kharaka et al., 2010). Although these approaches all yield useful information for assessing the geochemical outcomes of increased CO<sub>2</sub> in freshwater aquifers and their effects on drinking-water quality, they exclude the dynamic interplay of local hydrologic conditions on geochemistry.

For example, few, if any, researchers have included the possibility of dedolomitization in their assessments. This well-documented process (also known as *incongruent dissolution*) is widespread, occurring in aquifers around the world including in China (Ma et al., 2011), the Middle East (El-Naqa et al., 2007; Matter et al., 2005), the United States (Raines and Dewers, 1997; Saunders and Toran, 1994; Deike, 1990), Canada (Stotler et al., 2011; Fu et al., 2008), the Mediterranean (Lorite-Herrera et al., 2008; Capaccioni et al., 2001), and Europe (Zeeh et al., 2000). Dedolomitization occurs under a variety of sustained and episodic environmental conditions that produce mixing of dilute and concentrated Ca-rich waters in the presence of calcite and dolomite (Appelo and Postma, 2007; Back and Baedeker, 1989; Back et al., 1979, 1983; Bischoff et al., 1994; Hanshaw and Back, 1985; Pacheco and Szocs, 2006; Plummer and Back, 1980). Input of calcium ions via mixing with CaSO<sub>4</sub>-type waters has been documented to occur through dissolution of interbedded gypsum (Cardenal et al., 1994; Plummer et al., 1990), incorporation of CaSO<sub>4</sub> waters into limestone aquifers resulting from groundwater pumping (Appelo and Postma, 2007; Lopez-Chicano et al., 2001), or introduction of domestic leachates from fertilizers (Pacheco and Szocs, 2006).

Introduction of Ca<sup>2+</sup> into an aquifer can also result from input of Na<sup>+</sup>-rich waters, accompanied by cation exchange. For example, cation exchange driven by mixing has been documented at the freshwater/saltwater interface in the Netherlands and on the Nile delta (Appelo and Postma, 2007). Na<sup>+</sup> may also enter aquifers and drive cation exchange via leaching of NaCl brines deposited in unlined surface pits. In the SACROC (Scurry Area Canyon Reef Operators Committee) area of this study, as well as throughout Texas and many US oil-producing regions, significant volumes (on the order of millions of tonnes/year) of NaCl brines co-produced with oil from the 1940s through the 1960s were disposed of into unlined surface pits. In one example from 1961 (Burnitt et al., 1963), more than 9 million tonnes of co-produced saltwater was disposed of into unlined surface pits located directly on outcrops of the Ogallala Formation, which contains a major aquifer on the Texas High Plains. The result was direct contamination of large volumes (on the order of hundreds of millions of liters) of fresh groundwater (Ludwig, 1972). Large contaminant plumes are predicted to persist

for hundreds of years, adding slugs of salts to aquifers with each surface recharge event (Fryberger, 1972; Pettyjohn, 1982).

Appelo and Postma (2007) described the mass balance for the dedolomitization reaction driven by input of calcium ions by dissolution of gypsum or anhydrite as:



where 1 mol of dolomite dissolves for every 2 mol of calcite that precipitates. The equilibrium condition for this reaction at 25 °C is represented by Mg<sup>2+</sup>/Ca<sup>2+</sup> = 0.8, irrespective of the absolute values of these two ions in the system. Ratios of Mg<sup>2+</sup>/Ca<sup>2+</sup> < 0.8 therefore represent a system that favors dolomite dissolution and calcite precipitation (dedolomitization). The mass transfer necessary to conserve the equilibrium condition of Mg<sup>2+</sup>/Ca<sup>2+</sup> = 0.8 indicates that Mg<sup>2+</sup>, Ca<sup>2+</sup>, and SO<sub>4</sub><sup>2-</sup> should all increase during dedolomitization that is driven by dissolution of CaSO<sub>4</sub>.

## 1.2. Research objectives and approach

To test methodologies for CO<sub>2</sub> storage evaluation using shallow aquifers, we targeted a potable water source (Dockum aquifer) above a long-duration (>35 years) large-scale (~250 km<sup>2</sup>) engineered CO<sub>2</sub> injection site in western Texas. The SACROC oil field in Scurry County, currently operated by Kinder Morgan (KM), has injected CO<sub>2</sub> for enhanced oil recovery (EOR) since 1972, with approximately 50% recovery and recycling of injected CO<sub>2</sub>. Between 1972 and 2009, 175 Mmt (million metric tonnes) of CO<sub>2</sub> was injected, with 78 Mmt of CO<sub>2</sub> recovered (Kinder Morgan, personal communication, 2009). The balance of CO<sub>2</sub> is most likely sequestered within the deep-injection formation; there is no evidence that injectate CO<sub>2</sub> has entered the Dockum aquifer above SACROC (Smyth et al., 2009), and the site provides a field-based investigation of the potential of groundwater chemistry to be used as an early detection monitoring tool at this and other geological sequestration (GS) sites. We specifically target carbonate parameters that have gained attention in the literature owing to their apparent simplicity, cost effectiveness, and potential for widespread application at GS sites.

To accomplish our objective, we combined data from groundwater samples collected in the SACROC area (both inside and outside the boundaries of the SACROC oilfield) with regional historical data from the Texas Water Development Board (TWDB). We first identified overall geochemical trends in the aquifer and using major element variations. After major trends were identified, the response of carbonate parameters such as DIC, alkalinity, pH, and calcium to an input of CO<sub>2</sub> were assessed within the defined hydrogeochemical framework and compared with other types of environments.

## 2. Field site and geologic setting

SACROC oil field in Scurry County near Snyder, Texas, lies on the east edge of the Permian Basin in western Texas (Fig. 1). Oil production is from the Pennsylvanian/Permian Cisco and Canyon Reef Formations at a depth of about 2050 m (Anderson, 1954; Olien and Olien, 1982). Oil-bearing carbonates are overlain by salt, anhydrite, dolomite, limestone, and redbeds deposited in a variety of environments ranging from subtidal to supratidal (Gustavson, 1986). The overlying Triassic Dockum Group houses the potable water source that is investigated in this study.

Triassic sediments of the Dockum Group can be divided into upper and lower sections: the Lower Dockum, containing braided-stream, channel-related facies and overbank deposits, and the overlying, finer-grained Upper Dockum, dominated by floodplain and lacustrine muds and silts (Ashworth and Hopkins, 1995; Ewing et al., 2008; McGowen et al., 1979). Although mostly buried

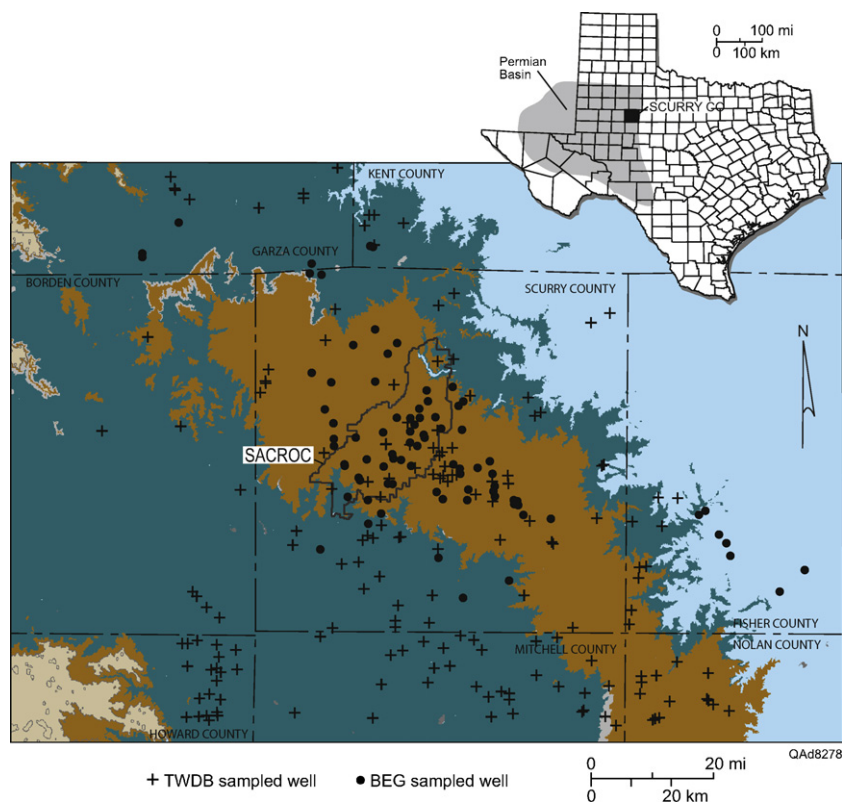


**Fig. 1.** Location of the SACROC oil field in Scurry County, Texas, on the east edge of the Permian Basin. The oil field lies on a remnant of Ogallala Formation (Eo) surrounded by outcrops of the Dockum Formation (TrD), which houses the aquifer of interest. Undifferentiated Permian formations (P) outcrop to the east. Sample locations are shown.

beneath sediments of the overlying Quaternary Blackwater Draw and Eocene Ogallala Formations in the Southern High Plains (SHP) to the west, the Dockum Group is the predominant outcropping unit in the Rolling Plains to the east. The exception is in the field area in Scurry County where the Upper Dockum has been eroded and a unique remnant of overlying Ogallala trends NW-SE from Garza to Nolan County (Fig. 1).

Although not used as a major water resource, the Dockum is locally important, serving as the source of local public water supply, irrigation for farming, livestock management, and oil-field operations (Bradley and Kalaswad, 2003). Groundwater in the Dockum Group is fresh to brackish and is locally impacted by dissolution of evaporite deposits in underlying Permian formations (Bradley and Kalaswad, 2003; Dutton, 1989). This impact is due to interaction between two regional aquifers which include (1) the SHP aquifer residing in Tertiary Ogallala and Triassic Dockum sediments down to the evaporite-bearing Permian strata (Richter and Kreitler, 1986), and (2) the underlying Paleozoic “deep basin brine” aquifer (DBB) that is separated from the overlying SHP aquifer by the Permian evaporite aquitard composed of halite, anhydrite, carbonate, and mudstone (Bassett et al., 1981; Jorgensen et al., 1988).

Flow within both aquifers is predominantly eastward (McNeal, 1965), with discharge points for the DBB east of the Texas Panhandle in north-central Texas (Jorgensen et al., 1988) and discharge points for the SHP aquifer in the Rolling Plains near the SACROC study area. Potentiometric pressures of the Dockum Group aquifer in some areas indicate the potential for downward flow into the upper part of the evaporite aquitard (Fink, 1963), causing a zone of dissolution referred to as a *salt dissolution zone*. Meteoric groundwater percolating upward into the updip Permian halite deposits moves eastward along highly transmissive dolomite and gypsum layers, discharging in topographically low areas (Simpkins and Fogg, 1982; Gustavson et al., 1980). These mixed waters are

transported through fractures from the dissolution zone to the surface, interacting with freshwater along the way (Fink, 1963; Jorgensen et al., 1988). Salt springs attributed to dissolution of underlying Permian sequences of gypsum, halite, and dolomite are well documented north of Scurry County in Garza, Kent, and Stonewall Counties (Richter and Kreitler, 1986; Richter et al., 1990; Stevens, 1974).

### 3. Materials and methods

#### 3.1. Sample collection and analyses

Approximately 100 fresh to slightly saline groundwater samples from the Triassic-age Dockum Group and the Paleocene-Eocene Ogallala Formation and 8 samples from Permian-age evaporite-bearing sandstones were collected from 59 private water wells (15–150 m deep) and 1 spring during 5 water sampling trips between June 2006 and November 2008. Ten samples of brines, co-produced from the 1800 to 2100 m injection/production zone were also analyzed. Additional geochemical data on co-produced brines were provided by KM, and historical records for Dockum and Permian water geochemistry collected by the TWDB between 1956 and 2008 from eight Texas counties were also added to the data set. Two samples of Dockum drill cuttings from depth intervals of 137 to 140 m and 112 to 116 m were examined for mineralogy using scanning electron microscopy (SEM) with the aid of an energy-dispersive X-ray system.

Samples from the water wells and spring were analyzed in the field for alkalinity, temperature, pH, specific conductivity, and dissolved oxygen. Major cations and trace metals were analyzed at Los Alamos National Laboratory by inductively coupled plasma-optical emission spectrometry (ICP-OES) and inductively coupled plasma-mass spectrometry (ICP-MS) using US Environmental Protection

Agency (EPA) approved analytical methods 200.7 and 200.8 (US EPA, 1994, 2001). Inorganic anion samples were analyzed by ion chromatography (IC) following EPA approved analytical method 300.0 (US EPA, 1993). Total dissolved organic carbon (DOC) and total dissolved inorganic carbon (DIC) were analyzed using combustion according to EPA method 415.1 (US EPA, 1999). Analytical data were evaluated using standard graphical and statistical tests, including regression and correlation approaches.

### 3.2. Sensitivity analyses

To understand how systems react to CO<sub>2</sub> and to discern the geochemical parameters most useful for monitoring GS sites, two types of analyses were developed: one that addresses how carbonate parameters will respond to different inputs of CO<sub>2</sub> within a given system and one that addresses the range of geochemical responses that would arise from geologic variability among sites. Both analyses use the response of carbonate parameters such as calcite and dolomite dissolution, DIC, HCO<sub>3</sub><sup>-</sup>, pH, and Ca<sup>2+</sup> to variations in CO<sub>2</sub>.

The first analysis determines the sensitivity of the Dockum aquifer above SACROC to different magnitudes of CO<sub>2</sub> input. This approach achieves two important goals: (1) to illustrate the magnitude of CO<sub>2</sub> input that would be necessary to discern a leakage signal from background noise at the SACROC site and (2) to evaluate the sensitivity of individual carbonate parameters to CO<sub>2</sub> within that system. If the system is sensitive to CO<sub>2</sub> input, geochemical parameters may be useful for monitoring because they would signal a leak in its early stages, providing greater options for protecting resources and/or remediation.

The second type of analysis considers the degree to which hydrogeologic variability can affect how carbonate parameters behave in the presence of CO<sub>2</sub>. This analysis considers the importance of understanding the specific hydrogeochemical characteristics of each aquifer that exists over a GS site, evaluates the importance of detailed characterization of each aquifer system, and determines the degree to which assumptions can be made on the basis of small data sets. For example, if the magnitude and direction of change of geochemical parameters are similar in any environment, these parameters will be useful for monitoring GS sites. If, however, site-specific conditions create wide-ranging effects and outcomes, their usefulness is decreased because intricate and costly characterizations at each site would be necessary.

Geochemical change upon addition of CO<sub>2</sub> into an aquifer is quantified by calculating the percent difference between the concentrations of the geochemical parameter before and after adding CO<sub>2</sub> into a system on the basis of the following equation:

$$\% \text{ Change} = \left| \frac{x1 - x2}{x1} \right| \times 100, \quad (2)$$

where  $x1$  is the beginning composition of the parameter being analyzed and  $x2$  is the ending composition of that parameter after CO<sub>2</sub> input. This type of analysis identifies the response of the system and forms the basis for comparing the sensitivity of individual geochemical parameters.

A similar approach was used to estimate how various aquifers with site-specific geochemical characteristics reacted to CO<sub>2</sub> input, providing information on the error that would result, for example, if the simple model of calcite dissolution were assumed in an aquifer that was experiencing dedolomitization. In this case, it is appropriate to use the equation for percent error:

$$\% \text{ Error} = \frac{\text{Assumed} - \text{Actual}}{\text{Actual}} \times 100, \quad (3)$$

where *Assumed* is the value calculated under the assumption of calcite dissolution and *Actual* is the value that would be expected from

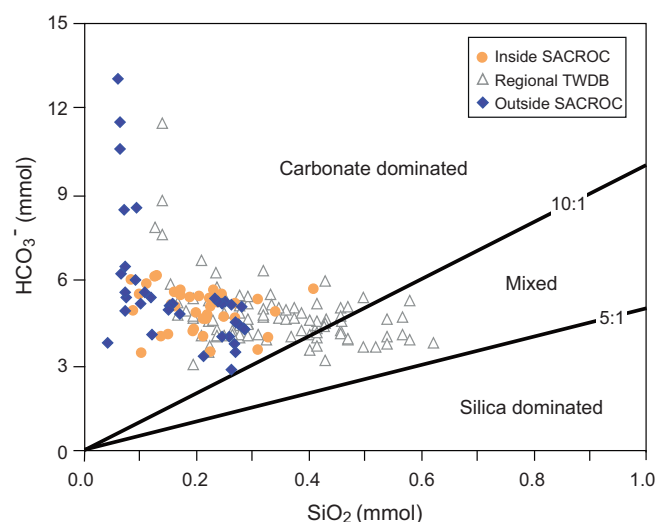


Fig. 2. Plot showing the relative influences of carbonate and silicate geochemistry in the Dockum aquifer near SACROC.

our model under dedolomitization. Unlike the percent-difference calculation in Eq. (2), this result will give a directional analysis, indicating whether the error would underestimate or overestimate the actual value.

## 4. Results and discussion

### 4.1. Sediment reactivity in the Dockum formation

Dockum aquifer sediments are predominantly siliciclastic, with small amounts (1%) of diagenetic and detrital calcite. Visual inspection of Dockum well cuttings collected from SACROC indicates a general composition of 60–80% quartz, 10–20% feldspar, 15% dark rock fragments, and minor carbonate cements. Results from SEM analyses show mineralogical content of quartz > K-feldspar > albite > dolomite > calcite. Quartz grains show no evidence of overgrowth or corrosion; however, feldspars show limited dissolution features. Clay, mostly smectite, coats most mineral grains. Dolomite (5%) occurs as ubiquitous rhombic crystals that often exhibit corrosion, suggesting dissolution.

Degree of influence of carbonate minerals in the predominantly siliciclastic Dockum aquifer was assessed using the relative abundances of SiO<sub>2</sub> and HCO<sub>3</sub><sup>-</sup> after Hounslow (1995). This method uses an arbitrary boundary of HCO<sub>3</sub><sup>-</sup>/SiO<sub>2</sub> < 5 to indicate dominance of silicate weathering and a ratio > 10 to indicate dominance of carbonate weathering. Data collected near SACROC and from the TWDB database (Fig. 2) show that, in spite of the volumetric dominance of silicates in the Dockum, samples are geochemically dominated by carbonate weathering. Regional data (shown as open triangles) also indicate the same importance of carbonate geochemistry, with a relatively minor influence of silicate weathering most likely representing feldspar dissolution. Overall, these geochemical relationships suggest that even small amounts of carbonate in an aquifer (1–5% in this case) may yield geochemical conditions receptive to changes in CO<sub>2</sub>, supporting the hypothesis that carbonate parameters may be useful indicators of leakage. This conclusion is in direct opposition to that of Wilkin and DiGiulio (2010), who argued that a quartz-rich aquifer would be nonreactive.

### 4.2. Major element trends

Piper diagrams (Piper, 1944) are common graphical tools for defining water types and the geochemical trends that result

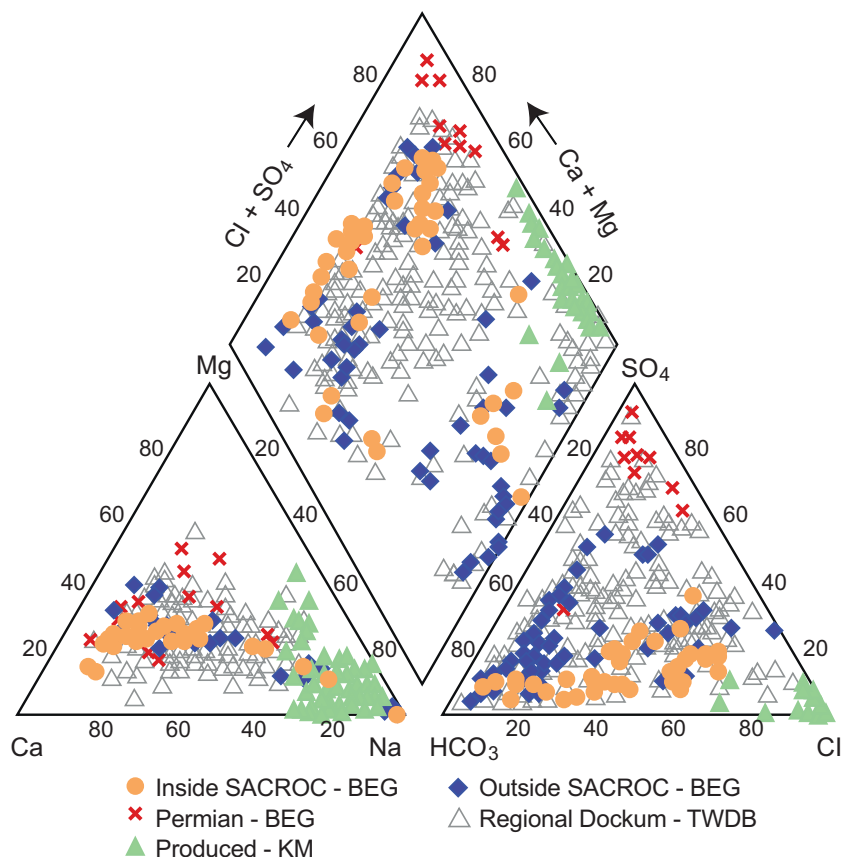


**Fig. 3.** Piper diagram showing compositions of samples from Dockum and Permian formations collected by the BEG during the study. Also shown are analyses provided by Kinder Morgan for produced brines and historical Dockum analyses furnished by the TWDB.

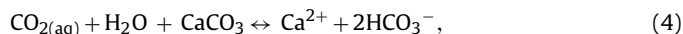
from mineral reactions, mixing among different waters, and ion exchange. Normalized values for major cations (lower-left triangle), anions (lower-right triangle), and a combination of the two (central diamond) were used to assess the major geochemical influences on the Dockum (Fig. 3). Dockum samples plot in all quadrants of the piper diagram, indicating a geochemical environment with many influences. As expected, Permian waters that reside in gypsum-containing formations plot as CaSO<sub>4</sub>-type waters. Waters co-produced with oil at SACROC are predominantly NaCl type. General trends on the anions triangle indicate two types of mixing: most (64%) samples outside SACROC appear to trend toward Permian compositions, whereas samples inside SACROC (and a few [36%] outside SACROC) appear to trend toward produced-water compositions indicating that variable amounts of mixing of Dockum water with Permian and co-produced brines affect the geochemistry of the Dockum at SACROC.

A trend stretching from Na<sup>+</sup> to Ca<sup>2+</sup> on the cation triangle further suggests that input of NaCl brines into the Dockum results in the exchange of Na<sup>+</sup> for Ca<sup>2+</sup> on exchange sites. In the case of SACROC, the exchange of Na<sup>+</sup> in solution for Ca<sup>2+</sup> sorbed to clays is fueled by mixing of Dockum and produced waters. Therefore, two mechanisms exist by which calcium ions are added to the shallow groundwater system: one, a natural process inherent to the regional system (mixing with CaSO<sub>4</sub>-type waters in the salt dissolution zone), and the other resulting from land-use practices (mixing with co-produced brines and cation exchange). Evidence that both processes are at work can be seen in relatively weak co-variation ( $R^2 = 0.0797$ ) between Ca<sup>2+</sup> and SO<sub>4</sub><sup>2-</sup> for all the data evaluated in the study that strengthens significantly ( $R^2 = 0.8716$ ) when the NaCl component is added and cation exchange is considered (Fig. 4). A general decrease in Cl<sup>-</sup> with depth (not shown) indicates that

NaCl input is likely from historical disposal of brine into surface pits rather than from brine migrating from the deep production reservoir.

#### 4.3. Dedolomitization and CO<sub>2</sub> input

The process of dedolomitization in the Dockum aquifer near SACROC is indicated by co-variation between Mg<sup>2+</sup> (an indicator of dolomite dissolution) and SO<sub>4</sub><sup>2-</sup> (an indicator of Ca<sup>2+</sup> input) with Mg<sup>2+</sup>/Ca<sup>2+</sup> < 0.8 (Fig. 5). An environment that is undergoing dedolomitization is very different from an environment that experiences simple calcite dissolution. Whereby calcite dissolution is driven by CO<sub>2</sub> according to the reaction.



dedolomitization is driven by calcium ions, which combine with carbonate supplied by dolomite dissolution to form calcite (Eq. (1)). The driving forces (reactants) and outcomes (products) of these two environments are different, illustrating the potential importance of defining the system before predicting the effects of CO<sub>2</sub>.

With the overall geochemical processes in Dockum aquifer system defined, the PHREEQC code (Parkhurst and Appelo, 1999) was used to constrain the role of CO<sub>2</sub> in a system dominated by dedolomitization rather than calcite dissolution. During calcite dissolution fueled by CO<sub>2</sub> (Eq. (4)), 1 mol of Ca<sup>2+</sup> and 2 mol of HCO<sub>3</sub><sup>-</sup> are produced, and data will trend along a line with a slope of 0.5 on a plot of Ca<sup>2+</sup> versus HCO<sub>3</sub><sup>-</sup> (arrow labeled as “Calcite dissolution” in Fig. 6). As expected, data do not follow calcite dissolution trends but, rather, fall within a range of trends modeled for dedolomitization under several conditions of constant PCO<sub>2</sub>. These trends were constructed by mixing 25 mmol of CaSO<sub>4</sub> to Dockum water initially

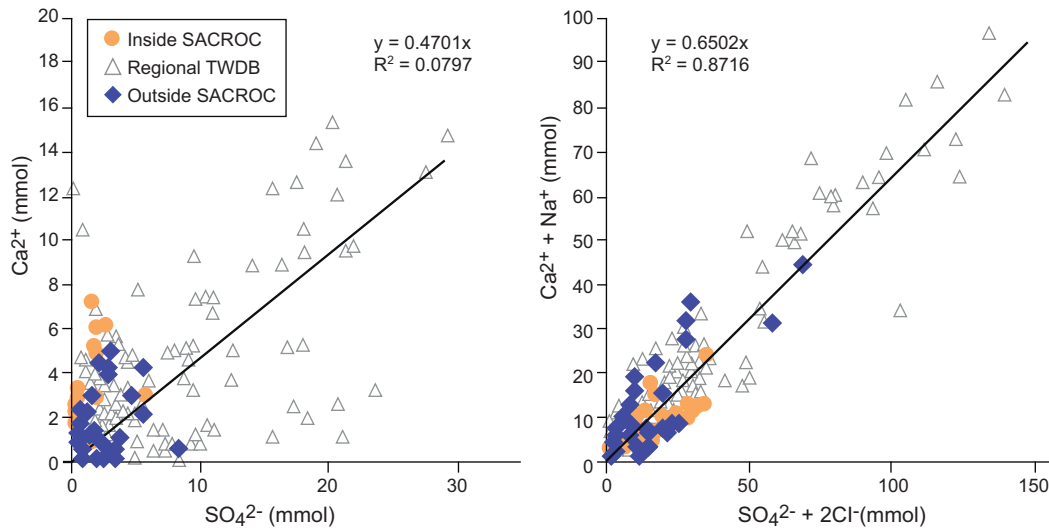


**Fig. 4.** Co-variation of  $\text{Ca}^{2+}$  with  $\text{SO}_4^{2-}$  (left) is not particularly strong, indicating  $\text{Ca}^{2+}$  is not solely supplied to the system by mixing with Permian  $\text{CaSO}_4$  waters. Addition of a NaCl produced water component with cation exchange (right) shows even stronger correlation, indicating both processes contribute to the input of calcium ions to the shallow aquifer.

in equilibrium with calcite and dolomite at various fixed  $\text{PCO}_2$ . Data correspond to these trends and generally lie within the boundaries defined by the range of constant  $\text{PCO}_2$  from  $10^{-2.7}$  to  $10^{-1.5}$  (Fig. 6).

During dedolomitization under constant  $\text{PCO}_2$ , geochemical evolution progresses from high to low  $\text{HCO}_3^-$  and from low to high  $\text{Ca}^{2+}$ . This progression is in contrast to the trend for calcite dissolution, which is from low to high  $\text{HCO}_3^-$  and  $\text{Ca}^{2+}$ . The presence of dissolved bicarbonate in the initial solution slows dolomite dissolution in the early stages of reaction by supplying some anions necessary for calcite precipitation, after which dissolved bicarbonate and calcium are quickly used, resulting in decreasing  $\text{HCO}_3^-$  and relatively steady  $\text{Ca}^{2+}$  concentrations. As the dissolved bicarbonate in the initial water is consumed, dolomite dissolves and calcite precipitates, and the kinetics of dissolution/precipitation

reactions control ion concentrations in the water. If the system re-equilibrates to a higher constant  $\text{PCO}_2$  under the normal aquifer conditions observed at the study site ( $\text{PCO}_2$  from  $10^{-2.7}$  to  $10^{-1.5}$ ), the mass of dolomite dissolution increases, the mass of calcite precipitation decreases,  $\text{HCO}_3^-$  increases, and pH decreases, all at higher constant  $\text{PCO}_2$ . Without knowledge of this system, we might wrongly assess that high bicarbonate samples ( $> \sim 10$  mmol) are anomalously impacted by  $\text{CO}_2$ . However, with the knowledge that the system is undergoing dedolomitization in response to complex mixing and cation exchange relationships, we understand that these samples are actually the least “evolved” or reacted in the system.

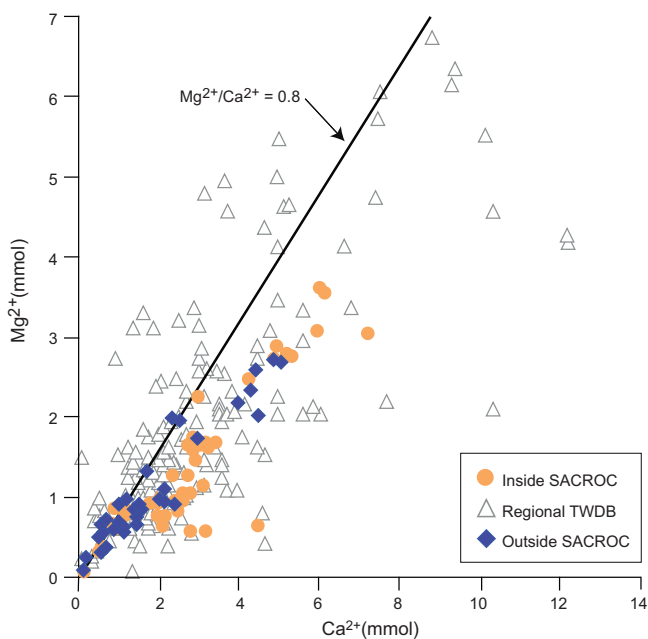


**Fig. 5.** Co-variation of  $\text{Mg}^{2+}$  and  $\text{Ca}^{2+}$  indicates a chemical driving force for dedolomitization.

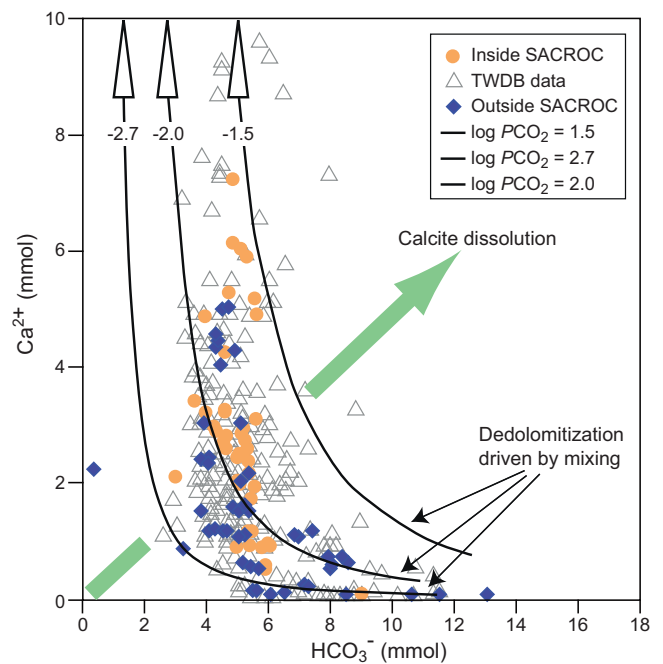


**Fig. 6.** Modeling results for evolution of  $\text{Ca}^{2+}$  and  $\text{HCO}_3^-$  during calcite dissolution and dedolomitization. Modeled curves for dedolomitization under constant  $\text{PCO}_2$  are shown for  $10^{-1.5}$ ,  $10^{-2.0}$ , and  $10^{-2.7}$ .

#### 4.4. Sensitivity of the system to CO<sub>2</sub> input

With the geochemical system defined, sensitivity of the system to CO<sub>2</sub> input can be predicted. When the data in Fig. 6 are visually compared with the modeled trends for constant PCO<sub>2</sub>, the data can be perceived to trend toward higher PCO<sub>2</sub> with geochemical evolution. For example, most samples with relatively low Ca<sup>2+</sup> of about 2 mmol cluster near an average modeled constant PCO<sub>2</sub> trend of about 10<sup>-2</sup>; however, more geochemically evolved samples with higher Ca<sup>2+</sup> concentrations of about 7 mmol, cluster near higher modeled PCO<sub>2</sub> of 10<sup>-1.5</sup>, suggesting that CO<sub>2</sub> is building in the system.

The observed phenomenon of increasing PCO<sub>2</sub> could result from CO<sub>2</sub>-EOR practices; however, no geochemical distinction has been observed between samples collected inside and outside SACROC that would suggest impact from CO<sub>2</sub> injection. In addition, modern data collected during the study both inside and outside SACROC show no geochemical distinction from historical regional data collected by TWDB from areas spatially and/or temporally removed from CO<sub>2</sub> injection. Groundwater quality inside SACROC is found to not be significantly degraded when compared against EPA drinking water standards (Smyth et al., 2009). Redox reactions producing HCO<sub>3</sub><sup>-</sup>, especially sulfate reduction, may play a role; however, aquifer conditions were highly oxidizing. We conclude that increases in PCO<sub>2</sub> represent normal system degassing during dedolomitization.

To simulate the perturbations that would occur if the potable aquifer were to receive CO<sub>2</sub> from the storage reservoir as the result of a leak, we performed a sensitivity analysis based in the system model constructed from the field data at SACROC. In the case of leakage into an aquifer experiencing dedolomitization, two mass transfers into the aquifer occur simultaneously and affect the intricate interplay between HCO<sub>3</sub><sup>-</sup> and Ca<sup>2+</sup>: (1) mass transfer of Ca<sup>2+</sup> from mixing and/or cation exchange and (2) mass transfer of CO<sub>2</sub> from a simulated leak. Ca<sup>2+</sup> input is essentially a function of the hydrodynamic factors producing mixing and is assumed to be a steady-state process for each environment that is modeled. With a constant rate of mixing and thus constant mass flux of Ca<sup>2+</sup> into the system, a leakage signal can be modeled as an increase in CO<sub>2</sub> input, which, when compared with a defined steady influx of Ca<sup>2+</sup>, manifests as an increase in CO<sub>2</sub>/Ca<sup>2+</sup>. Alternately, this ratio can also be varied and used to represent different conditions of mixing that exist in different aquifers having different hydrodynamics. Because CO<sub>2</sub>/Ca<sup>2+</sup> is independent of absolute fluxes, the ratio can be used to represent a variety of different environmental fluxes and conditions.

The initial sensitivity simulation was structured to define the amount of CO<sub>2</sub> needed to create the observed CO<sub>2</sub> increase exhibited in the natural system as defined by the SACROC field data in Fig. 6. A starting water composition was chosen at the point in the system where PCO<sub>2</sub> shifts to higher values (about 4.5 mmol HCO<sub>3</sub><sup>-</sup> and 1 mmol Ca<sup>2+</sup>). The ending composition was chosen to represent the magnitude of the shift that was visually observed in the dataset (about 5 mmol HCO<sub>3</sub><sup>-</sup> and 9 mmol Ca<sup>2+</sup>). Model results indicate that the shift toward higher PCO<sub>2</sub> in the field data is consistent with the addition of 1.5 mmol of CO<sub>2</sub> and 15 mmol CaSO<sub>4</sub> at a CO<sub>2</sub>/Ca<sup>2+</sup> ratio of 0.1.

CO<sub>2</sub> was then added to the system using randomly chosen CO<sub>2</sub>/Ca<sup>2+</sup> ratios of 0.1, 0.5, 1, 2, and 10 to investigate how different mixing conditions manifested similar CO<sub>2</sub> inputs. The evolutionary trends for the varying CO<sub>2</sub>/Ca<sup>2+</sup> ratios are shown in Fig. 7 (broken lines), along with calcite dissolution (solid line) for comparison purposes. Results show trends different from the evolution of waters modeled under constant PCO<sub>2</sub> (Fig. 6). In systems with less input from mixing (i.e., with greater CO<sub>2</sub>/Ca<sup>2+</sup>), reaction pathways shifted toward higher HCO<sub>3</sub><sup>-</sup> and lower Ca<sup>2+</sup> and more closely mimicked

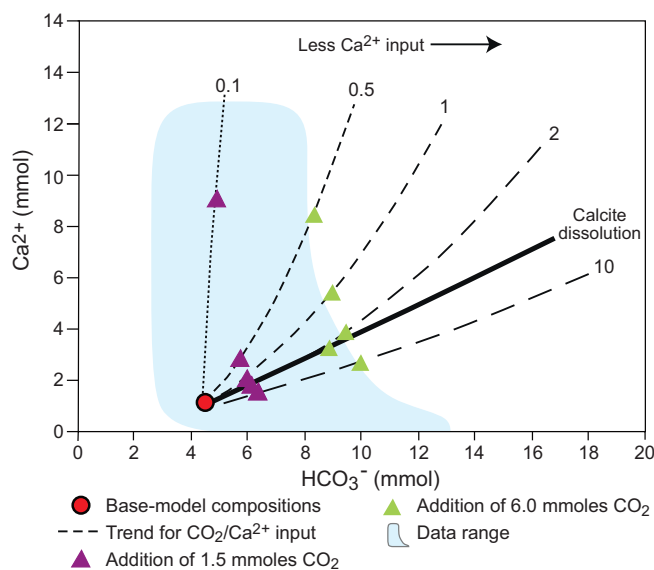


Fig. 7. Results of CO<sub>2</sub> sensitivity modeling. Shaded area represents background geochemical variation in the aquifer. Beginning composition for all models is denoted by a red dot. Ending compositions are shown by triangles. Responses of the system to various mass inputs of CO<sub>2</sub> under different mixing conditions are shown.

calcite dissolution, although the modeled simulation predicted that dolomite continued to dissolve and calcite continued to precipitate.

Points of equal CO<sub>2</sub> input (1.5 mmol and 6 mmol) into each environment defined by a specific relative rate of mass transfer (CO<sub>2</sub>/Ca<sup>2+</sup>) and for straight calcite dissolution are shown by solid triangles in Fig. 7. Model output is presented (Table 1) for addition of 1.5, 6, and 50 mmol of CO<sub>2</sub>. The high margin (50 mmol) was randomly chosen to represent an order of magnitude higher input of CO<sub>2</sub> than was modeled using the SACROC data. Background geochemical variability at SACROC is represented by the spread of regional data collected outside SACROC, as indicated by the shaded area in Fig. 7. Sensitivity analysis shows that 6 mmol of CO<sub>2</sub> is necessary to achieve Ca<sup>2+</sup> and HCO<sub>3</sub><sup>-</sup> compositions outside of background concentrations for this specific system. Also evident from the simulations is that a system undergoing calcite dissolution will be slightly less sensitive to CO<sub>2</sub> input than one undergoing dedolomitization.

To understand the significance of 6 mmol of CO<sub>2</sub> input into an aquifer with regard to a leakage rate from a storage formation, we performed a mass balance exercise using anthropogenic emissions expected from a 500-MW (Megawatt) power plant, which is assumed to produce and store up to 3 million tonnes/year of CO<sub>2</sub> (MIT Interdisciplinary Study, 2010). Assumptions are: (1) a saturated aquifer thickness of 60 m with a porosity of 0.30, (2) an area of consideration within the aquifer of 1 ha (10<sup>4</sup> m<sup>2</sup>), and (3) that any CO<sub>2</sub> leaked from the storage reservoir is instantaneously and equally distributed throughout the area of consideration. We have discerned, through careful inspection and modeling of the hydrochemical environment at SACROC, that the CO<sub>2</sub> concentration necessary to produce a geochemical signature above background conditions is 6 mmol/L. This equates to 4.75 × 10<sup>6</sup> g of CO<sub>2</sub> within the 1-ha area and represents a 0.001% leakage rate of the total yearly output from a 500-MW power plant. The system appears sensitive enough to detect a relatively small leak; however, because the model conservatively assumes instantaneous distribution throughout the area of consideration, the actual measurement of change will depend on the type and areal distribution of the leak. For example, if the leak enters the aquifer as a point source, the geochemical signal will be strong but difficult to locate spatially. If the leak enters the aquifer more diffusely, the geochemical signal will be weaker but easier to

**Table 1**  
Model output for addition of varying amounts of CO<sub>2</sub> into different carbonate systems. Starting composition is shown and is the same for each simulation.

| CO <sub>2</sub> :Ca <sup>2+</sup> | CO <sub>2</sub> added (mmol) | Ca <sup>2+</sup> added (mmol) | Δ calcite (mmol) | Δ dolomite (mmol) | log PCO <sub>2</sub> (mmol) | DIC (mmol) | HCO <sub>3</sub> <sup>-</sup> (mmol) | pH (mmol) | Mg <sup>2+</sup> (mmol) | Ca <sup>2+</sup> (mmol) |
|-----------------------------------|------------------------------|-------------------------------|------------------|-------------------|-----------------------------|------------|--------------------------------------|-----------|-------------------------|-------------------------|
| <b>1.5 mmol CO<sub>2</sub></b>    |                              |                               |                  |                   |                             |            |                                      |           |                         |                         |
| Start composition                 | n/a                          | n/a                           | n/a              | n/a               | -2.36                       | 4.87       | 4.60                                 | 7.77      | 0.69                    | 1.06                    |
| 0.1                               | 1.5                          | 15                            | 14.30            | -7.25             | -1.44                       | 6.61       | 4.88                                 | 6.84      | 7.94                    | 9.05                    |
| 0.5                               | 1.5                          | 3                             | 3.01             | -1.81             | -1.58                       | 6.97       | 5.73                                 | 7.07      | 2.50                    | 2.86                    |
| 1                                 | 1.5                          | 1.5                           | 1.60             | -1.15             | -1.62                       | 7.07       | 5.96                                 | 7.13      | 1.84                    | 2.11                    |
| 2                                 | 1.5                          | 0.75                          | 0.89             | -0.83             | -1.65                       | 7.13       | 6.09                                 | 7.17      | 1.52                    | 1.75                    |
| 10                                | 1.5                          | 0.15                          | 0.33             | -0.58             | -1.68                       | 7.19       | 6.22                                 | 7.22      | 1.27                    | 1.46                    |
| Calcite dissolution               | 1.5                          | n/a                           | -0.69            | n/a               | -1.62                       | 7.06       | 5.98                                 | 7.14      | 0.69                    | 1.76                    |
| <b>6 mmol CO<sub>2</sub></b>      |                              |                               |                  |                   |                             |            |                                      |           |                         |                         |
| Start composition                 | n/a                          | n/a                           | n/a              | n/a               | -2.36                       | 4.87       | 4.60                                 | 7.77      | 0.69                    | 1.06                    |
| 0.1                               | 6                            | 60                            | 56.1             | -28.7             | -0.91                       | 12.30      | 6.50                                 | 6.39      | 29.40                   | 33.70                   |
| 0.5                               | 6                            | 12                            | 11.3             | -6.7              | -0.98                       | 12.90      | 8.32                                 | 6.61      | 7.39                    | 8.44                    |
| 1                                 | 6                            | 6                             | 5.68             | -4.02             | -1.02                       | 13.20      | 8.97                                 | 6.69      | 4.71                    | 5.40                    |
| 2                                 | 6                            | 3                             | 2.86             | -2.71             | -1.04                       | 13.40      | 9.44                                 | 6.74      | 3.40                    | 3.91                    |
| 10                                | 6                            | 0.6                           | 0.602            | -1.7              | -1.07                       | 13.70      | 9.95                                 | 6.80      | 2.39                    | 2.75                    |
| Calcite dissolution               | 6                            | n/a                           | -2.34            | n/a               | -1.02                       | 13.20      | 9.12                                 | 6.71      | 0.69                    | 3.40                    |
| <b>50 mmol CO<sub>2</sub></b>     |                              |                               |                  |                   |                             |            |                                      |           |                         |                         |
| Start composition                 | n/a                          | n/a                           | n/a              | n/a               | -2.36                       | 4.87       | 4.60                                 | 7.77      | 0.69                    | 1.06                    |
| 0.1                               | 50                           | 500                           | 0.46             | -0.23             | 0.12                        | 61.90      | 11.80                                | 5.57      | 234.00                  | 275.00                  |
| 0.5                               | 50                           | 100                           | 0.09             | -0.05             | 0.05                        | 62.80      | 16.90                                | 5.84      | 50.90                   | 58.70                   |
| 1                                 | 50                           | 50                            | 0.05             | -0.03             | 0.03                        | 63.50      | 19.10                                | 5.92      | 28.10                   | 32.30                   |
| 2                                 | 50                           | 25                            | 0.02             | -0.02             | 0.02                        | 64.20      | 21.10                                | 5.99      | 16.80                   | 19.30                   |
| 10                                | 50                           | 5                             | 0.004            | -0.01             | 0.005                       | 65.40      | 23.90                                | 6.08      | 8.00                    | 9.27                    |
| Calcite dissolution               | 50                           | n/a                           | -8.64            | n/a               | 0.02                        | 63.50      | 20.80                                | 6.02      | 0.69                    | 9.70                    |

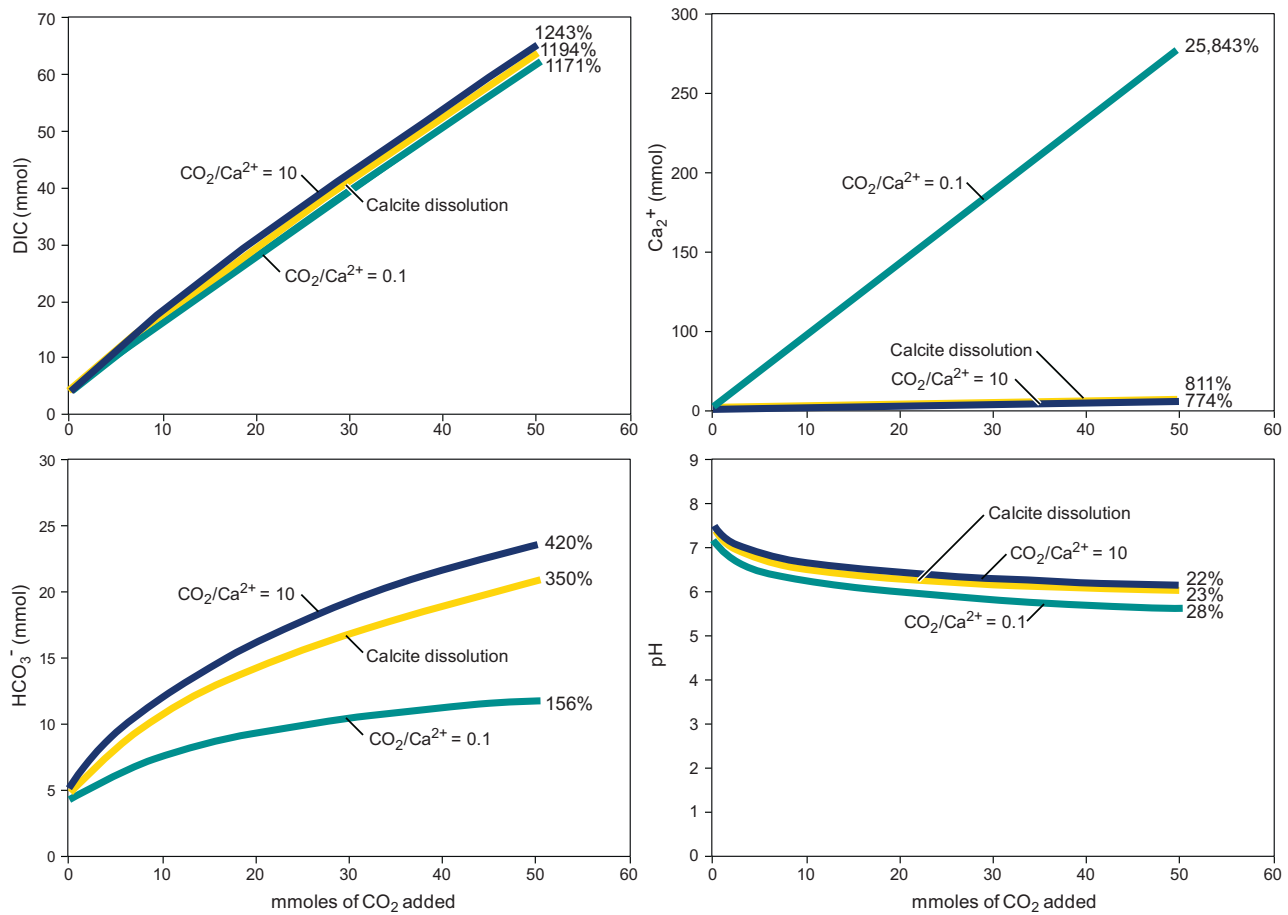


**Fig. 8.** Percent change from starting composition for various carbonate parameters during modeled input of CO<sub>2</sub> (x axis). Parameter responses for a range of environments undergoing dedolomitization and calcite dissolution are shown with values for percent change noted beside respective trends. DIC shows the highest and most predictable variability.

locate spatially. The calculation described herein is more applicable to the latter case.

To identify which carbonate parameter is best suited for monitoring at a variety of sites, how each parameter responds during carbonate dissolution and dedolomitization must be understood. The most desirable parameter will have the highest sensitivity to increasing CO<sub>2</sub> input (i.e., the largest change), and the magnitude and direction of its change should be similar, and, therefore, predictable, in any environment. The modeled responses of DIC, Ca<sup>2+</sup>, HCO<sub>3</sub><sup>-</sup>, and pH to increasing CO<sub>2</sub> input are presented in Fig. 8 for CO<sub>2</sub>/Ca<sup>2+</sup> = 0.1 and 10 and for calcite dissolution, representing the range of expected environmental responses. Percent change for

each parameter with increasing CO<sub>2</sub> input (calculated using Eq. (2)) is noted for each simulation.

Of the four parameters, DIC has the highest sensitivity with the largest and most consistent percent changes from the starting composition (1171%, 1194%, and 1243% for CO<sub>2</sub>/Ca<sup>2+</sup> = 0.1, calcite dissolution, and CO<sub>2</sub>/Ca<sup>2+</sup> = 10, respectively). Although Ca<sup>2+</sup> also shows relatively high sensitivity, its percent change is largely variable (ranging from 774% to 25,843%) and unpredictable and depends heavily on the flux of Ca<sup>2+</sup> into the system via mixing. Predicting this outcome necessitates knowledge of mixing relationships, which requires in-depth characterization of hydrodynamics, therefore disqualifying Ca<sup>2+</sup> as a useful global monitoring

**Table 2**  
Percent error that would result if a system undergoing dedolomitization were assessed assuming calcite dissolution.

| CO <sub>2</sub> :Ca <sup>2+</sup> | CO <sub>2</sub> added (mmol) | Ca <sup>2+</sup> added (mmol) | DIC (% error) | HCO <sub>3</sub> <sup>-</sup> (% error) | pH (% error) | Ca <sup>2+</sup> (% error) |
|-----------------------------------|------------------------------|-------------------------------|---------------|---|--------------|----------------------------|
| 6 mmol CO <sub>2</sub>            |                              |                               |               |   |              |                            |
| 0.1                               | 6                            | 60                            | -2.4          | -26.5                                   | -5.2         | 4160.9                     |
| 0.5                               | 6                            | 12                            | 2.4           | -5.9                                    | -1.9         | 971.0                      |
| 1                                 | 6                            | 6                             | 4.8           | 1.5                                     | -0.7         | 582.6                      |
| 2                                 | 6                            | 3                             | 6.3           | 6.8                                     | 0.0          | 392.8                      |
| 10                                | 6                            | 0.6                           | 8.7           | 12.6                                    | 0.9          | 246.4                      |
| 50 mmol CO <sub>2</sub>           |                              |                               |               |   |              |                            |
| 0.1                               | 50                           | 500                           | -2.5          | -43.3                                   | -7.5         | 33813.0                    |
| 0.5                               | 50                           | 100                           | -1.1          | -18.8                                   | -3.0         | 7276.8                     |
| 1                                 | 50                           | 50                            | 0.0           | -8.2                                    | -1.7         | 3972.5                     |
| 2                                 | 50                           | 25                            | 1.1           | 1.4                                     | -0.5         | 2334.8                     |
| 10                                | 50                           | 5                             | 3.0           | 14.9                                    | 1.0          | 1059.4                     |

parameter.  $\text{HCO}_3^-$  exhibits the next-greatest sensitivity (ranging from 156% to 420% change from initial composition), but with a highly variable magnitude. This variability is due to pH dependence of the distribution of carbonate species ( $\text{H}_2\text{CO}_3$ ,  $\text{HCO}_3^-$ ,  $\text{CO}_3^{2-}$ ) in natural waters, which complicates interpretation of  $\text{HCO}_3^-$  concentrations with regard to the mass of  $\text{CO}_2$  that has entered the aquifer. Relatively consistent magnitude and range of change are shown by the response of pH (28%, 23%, and 22% for  $\text{CO}_2/\text{Ca}^{2+} = 0.1$ , calcite dissolution, and  $\text{CO}_2/\text{Ca}^{2+} = 10$ , respectively), but the sensitivity of this parameter is quite small.

Similarly, the percent errors (calculated using Eq. (3)) that would be incurred using each parameter to assess a system undergoing dedolomitization under the assumption of calcite dissolution are presented in Table 2 for 6 and 50 mmol  $\text{CO}_2$  input. Errors for calcium concentrations are large (from 246% to 33,813%) and again disqualify this parameter as one useful for monitoring. Of the remaining parameters (DIC,  $\text{HCO}_3^-$ , and pH), errors are bidirectional, with some dedolomitization environments yielding parameter concentrations lower and some higher than expected from calcite dissolution.  $\text{HCO}_3^-$  shows the largest ranges in error (−26.5% to 12.6% for 6 mmol  $\text{CO}_2$  input and −43.3% to 14.9% for 50 mmol  $\text{CO}_2$  input). DIC (−2.4% to 8.7% and −2.5% to 3.0% for 6 and 50 mmol  $\text{CO}_2$  input, respectively) and pH (−5.2% to 0.9% and −7.5% to 1.0% for 6 and 50 mmol  $\text{CO}_2$  input, respectively) exhibit smaller ranges in error. Results indicate that changes due to  $\text{CO}_2$  input in an uncharacterized system would best be predicted and quantified using DIC as a monitoring parameter due to its high sensitivity to  $\text{CO}_2$  and predictable behavior in any hydrologic environment.

## 5. Conclusions

Carbonate geochemical parameters (e.g., pH,  $\text{Ca}^{2+}$ , and  $\text{HCO}_3^-$ ) are widely proposed as being suitable for shallow aquifer monitoring above carbon storage sites based on the assumption that calcite dissolution will result from  $\text{CO}_2$  leakage into an aquifer. A field study and modeling of the Dockum aquifer above the SACROC  $\text{CO}_2$ -enhanced oil recovery site indicates that calcite dissolution cannot be assumed because dedolomitization is the dominant hydrogeochemical process in this aquifer. Dedolomitization at SACROC is fueled by input of  $\text{Ca}^{2+}$  by two mechanisms: (1) a natural process inherent to the regional system which creates mixing of freshwater with  $\text{CaSO}_4$ -type waters in a salt dissolution zone, and (2) human-induced land-use practices that cause mixing of freshwater with co-produced brines resulting in cation exchange and release of  $\text{Ca}^{2+}$  into the aquifer. Although dedolomitization is a common process in aquifers worldwide, it has not been considered in predictions of how aquifers would respond to  $\text{CO}_2$ .

Sensitivity analyses of systems subject to dedolomitization and those subject to calcite dissolution suggest that both systems are significantly sensitive to  $\text{CO}_2$  input. The aquifer at SACROC would require an input of only 6 mmol  $\text{CO}_2$  to elevate geochemical concentrations of  $\text{HCO}_3^-$  and  $\text{Ca}^{2+}$  to levels above background, which is roughly equivalent to detecting a 0.001% leakage rate from a 500-MW power plant. However, parameters commonly suggested as leakage indicators in potable aquifers (pH,  $\text{HCO}_3^-$  and  $\text{Ca}^{2+}$ ) are variably sensitive to  $\text{CO}_2$  input and exhibit unpredictable behavior in a range of natural systems. Such behavior would therefore require detailed characterization of each aquifer above a  $\text{CO}_2$  storage site to develop monitoring criteria. Model results show that DIC is highly sensitive to  $\text{CO}_2$  and will react similarly and predictably in a variety of geologic environments undergoing dedolomitization and/or calcite dissolution. The implication for monitoring GS sites is that expensive characterization of fundamental geochemical processes may not be necessary for monitoring  $\text{CO}_2$  input in shallow aquifers if DIC is used a monitoring parameter.

## Acknowledgments

This work has been supported financially through the US Department of Energy (US DOE), National Energy Technology Laboratory (NETL) contract DE FG26-05NT42590, Southwest Regional Carbon Sequestration Partnership Program (RCSP), which was administered by New Mexico Tech with industry support from Kinder Morgan companies (KM). We greatly appreciate KM providing access to the SACROC oil-field site and cooperation of the many private landowners who allowed us to sample their water wells. In addition, this work could not have been conducted without logistical support in the field from KM, with special thanks to Nathan Mathis, whose field support greatly enhanced the project. Many thanks go to Michael Young for his extensive editorial input. We also wish to recognize the financial support of the Gulf Coast Carbon Center (GCCC) and Los Alamos National Laboratory for providing much of the analytical data from groundwater samples using RCSP funds.

## References

- Anderson, K.F., 1954. Petroleum-Engineering Study of Scurry Reef Reservoir, Scurry County. Petroleum Engineering, Texas.
- Appelo, C.A.J., Postma, D., 2007. Geochemistry. Groundwater and Pollution, Amsterdam, AA Balkema.
- Apps, J.A., Zhang, Y., Zheng, L., Xu, T., Birkholzer, J.T., 2009. Identification of thermodynamic controls defining the concentrations of hazardous elements in potable ground waters and the potential impact of increasing carbon dioxide partial pressure. Energy Procedia 1 (1), 1917–1924.
- Ashworth, J.B., Hopkins, J., 1995. Major and Minor Aquifers of Texas, Report 345. Texas Water Development Board, Austin.
- Assayag, N., Matter, J., Ader, M., Goldberg, D., Agrinier, P., 2009. Water-rock interactions during a  $\text{CO}_2$  injection field-test: implications on host rock dissolution and alteration effects. Chemical Geology 265 (1–2), 227–235.
- Bachu, S., Bennion, D.B., 2009. Experimental assessment of brine and/or  $\text{CO}_2$  leakage through well cements at reservoir conditions. International Journal of Greenhouse Gas Control 3 (4), 494–501.
- Back, W., Baedecker, M.J., 1989. Chemical hydrogeology in natural and contaminated environments. Journal of Hydrology 106 (1–2), 1–28.
- Back, W., Hanshaw, B.B., Pyle, T.E., Plummer, L.N., Weidie, A.E., 1979. Geochemical significance of groundwater discharge and carbonate solution to the formation of Caleta Xel Ha, Quintana Roo, Mexico. Water Resources Research 15 (6), 1521–1535.
- Back, W., Hanshaw, B.B., Plummer, L.N., Rahn, P.H., Rightmire, C.T., Rubin, M., 1983. Process and rate of dedolomitization: mass transfer and  $^{14}\text{C}$  dating in a regional carbonate aquifer. Geological Society of America Bulletin 94, 1415–1429.
- Bassett, R.L., Bentley, M.E., Simpkins, W.W., 1981. Regional groundwater flow in the Panhandle of Texas—a conceptual model. In: Gustavson, T.C., Bassett, R.L., Finley, R.J., Goldstein, A.G. (Eds.), Geology and Geohydrology of the Palo Duro Basin, Texas. Panhandle: A Report on the Progress of Nuclear Waste Isolation Feasibility Studies (1980). The University of Texas at Austin, Bureau of Economic Geology, Geological Circular 81-3, pp. 102–107.
- Bischoff, J.L., Juliá, R., Shanks, W.C., Rosenbauer, R.J., 1994. Karstification without carbonic acid: bedrock dissolution gypsum-driven dedolomitization. Geology 22, 995–998.
- Blum, J.D., Gazis, C.A., Jacobson, A.D., Chamberlain, C.P., 1998. Carbonate versus silicate weathering in the Raikhot watershed within the high Himalayan crystalline series. Geology 26, 411–414.
- Bradley, R.G., Kalaswad, S., 2003. The Groundwater Resources of the Dockum Aquifer in Texas. Texas Water Development Board, Report 359, 73 pp.
- Burnitt, S.C., Adams, J.B., Rucker, O.C., Porterfield, H.C., 1963. Effects of oil disposal of oil field brines on the quality and development of ground water in the Ogallala Formation. High Plains of Texas: Prepared for Texas Water Commission, public hearing held by Water Pollution Control Board, Austin, Texas.
- Capaccioni, B., Didero, M., Paletta, C., Salvadori, P., 2001. Hydrogeochemistry of groundwaters from carbonate formations with basal gypsiferous layers: an example from the Mt Catria-Mt Nerone ridge (Northern Appennines, Italy). Journal of Hydrology 253 (1–4), 14–26.
- Cardenal, J., Benavente, J., Cruz-Sanjulian, J.J., 1994. Chemical evolution of groundwater in Triassic gypsum-bearing carbonate aquifers. Journal of Hydrology 161, 3–30.
- Carroll, S., Hao, Y., Aines, R., 2009. Geochemical detection of  $\text{CO}_2$  in dilute aquifers. Geochimical Transactions 10, 4.
- Chang, K.W., Minkoff, S.E., Bryant, S.L., 2009. Simplified model for  $\text{CO}_2$  leakage and its attenuation due to geological structures. Energy Procedia 1 (1), 3453–3460.
- Deike, R.G., 1990. Dolomite dissolution rates and possible Holocene dedolomitization of water-bearing units in the Edwards aquifer, south-central Texas. Journal of Hydrology 112 (3–4), 335–373.
- Dutton, A.R., 1989. Hydrogeochemical processes involved in salt-dissolution zones, Texas Panhandle, USA. Hydrological Processes 3, 75–89.

- El-Naqa, A., Al-momani, M., Kilani, S., Hammouri, N., 2007. Groundwater deterioration of shallow groundwater aquifers due to overexploitation in Northeast Jordan. *Clean* 35 (2), 156–166.
- Ewing, J.E., Jones, T.L., Yan, T., Vreugdenhil, A.M., Fryar, D.G., Pickens, J.F., Gordon, K., Nicot, J.P., Scanlon, B.R., Ashworth, J.B., Beach, J., 2008. Groundwater Availability Model for the Dockum Aquifer, Texas Water Development Board Final Report.
- Fink, B.E., 1963. Ground-water Geology of Triassic Deposits, Northern Part of the Southern High Plains of Texas, High Plains Underground Water Conservation District No. 1, Rep. No. 163, p. 77.
- Fryberger, J.S., 1972. Rehabilitation of a Brine Polluted Aquifer. US Environmental Protection Agency, EPA-R2-82-014.
- Fu, Q., Qing, H., Bergman, K.M., Yang, C., 2008. Dedolomitization and calcite cementation in the Middle Devonian Winnipegosis Formation in Central Saskatchewan, Canada. *Sedimentology* 55, 1623–1642.
- Gasda, S., Nordbotten, J., Celia, M.A., 2009. Vertical equilibrium with sub-scale analytical methods for geological CO<sub>2</sub> sequestration. *Computational Geosciences* 13 (4), 469–481.
- Gustavson, T.C., 1986. Geomorphic development of the Canadian River Valley, Texas Panhandle: an example of regional salt dissolution and subsidence. *Geological Society of America Bulletin* 97 (4), 459–472.
- Gustavson, T.C., Bassett, R.L., Finley, R.J., Goldstein, A.G., Handford, C.R., McGowen, J.H., Presley, M.W., Baumgardner, R.W., Bentley Jr. M.E., Dutton, S.P., Griffin, J.A., Hoadley, A.D., Howard, R.C., McGookey, D.A., McGillis, K.A., Palmer, D.P., 1980. Geology and Geohydrology of the Palo Duro Basin, Texas Panhandle. The University of Texas at Austin, Bureau of Economic Geology Geological Circular 82-7, 212 pp.
- Hanshaw, B.B., Back, W., 1985. Deciphering hydrological systems by means of geochemical processes. *Hydrological Sciences Journal* 30 (2), 257–271.
- Hounslow, A.W., 1995. *Water Quality Data-Analysis and Interpretations*. Lewis Publishers, New York.
- IPCC, 2005. IPCC Special Report on Carbon Dioxide Capture and Storage. Prepared by Working Group III of the Intergovernmental Panel on Climate Change. In: Metz, B., Davidson, O., de Coninck, H.C., Loos, M., Meyer, L.A. (Eds.). Cambridge University Press, Cambridge, United Kingdom and New York, NY, USA, 442 pp.
- Jorgensen, D.G., Downey, J., Dutton, A.R., Maclay, R.W., 1988. Region 16, central non-glaciated plains. In: Back, W., Rosenshein, J.S., Seaber, P.R. (Eds.), *Hydrogeology*. Geological Society of America, The Geology of North America, pp. 141–156, O-2.
- Kharaka, Y.K., Thordsen, J.J., Kakouros, E., Ambats, G., Herkelrath, W.N., Beers, S.R., Birkholzer, J.T., Apps, J.A., Spycher, N.F., Zheng, L., Trautz, R.C., Rauch, H.W., Gullickson, K.S., 2010. Changes in the chemistry of shallow groundwater related to the 2008 injection of CO<sub>2</sub> at the ZERT field site, Bozeman, Montana. *Environmental Earth Sciences* 60 (2), 273–284.
- Lopez-Chicano, M., Bouamama, M., Vallejos, A., Pulido-Bosch, 2001. Factors which determine the hydrogeochemical behavior of karstic springs. A case study from the Betic Cordilleras, Spain. *Applied Geochemistry* 16, 1179–1192.
- Lorite-Herrera, M., Jimenez-Espinosa, R., Jimenez-Millan, J., Hisock, K.M., 2008. Integrated hydrochemical assessment of the Quaternary alluvial aquifer of the Guadalquivir River, southern Spain. *Applied Geochemistry* 23, 2040–2054.
- Lu, J., Partin, J.W., Hovorka, S.D., Wong, C., 2010. Potential risks to freshwater resources as a result of leakage from CO<sub>2</sub> geological storage: a batch-reaction experiment. *Environmental Earth Sciences* 60 (2), 335–348.
- Ludwig, A.H., 1972. *Water Resources of Hempstead, Lafayette, Little River, Miller, and Nevada Counties, Arkansas*. US Geological Survey Water-Supply Paper 1998, 41 pp.
- Ma, R., Wang, Y., Sun, Z., Zheng, C., Ma, T., Prommer, H., 2011. Geochemical evolution of groundwater in carbonate aquifers in Taiyuan, Northern China. *Applied Geochemistry* 26 (5), 884–897.
- Matter, J.M., Waber, H.N., Loew, S., 2005. Recharge areas and geochemical evolution of groundwater in an alluvial aquifer system in the Sultanate of Oman. *Hydrogeology Journal* 14, 203–224.
- McGowen, J.H., Granata, G.E., Seni, S.J., 1979. Depositional Framework of the Lower Dockum Group (Triassic), Texas Panhandle. The University Texas, Austin, Bureau of Economic Geology Report of Investigations No. 97, 60 pp.
- McNeal, R.P., 1965. Hydrodynamics of the Permian Basin. In: Young, A., Galley, J.E. (Eds.), *Fluids in Subsurface Environments*, vol. 4. American Association of Petroleum Geologists Memoir, pp. 308–326.
- Nicot, J.P., 2008. Evaluation of large-scale CO<sub>2</sub> storage on fresh-water sections of aquifers: an example from the Texas Gulf Coast Basin. *International Journal of Greenhouse Gas Control* 2 (4), 582–593.
- Olien, R.M., Olien, D.D., 1982. *Oil Booms: Social Change in Five Texas Towns*. University of Nebraska Press, Lincoln.
- Pacheco, F.A.L., Szocs, L., 2006. Dedolomitization reactions driven by anthropogenic activity on loess sediments, SW Hungary. *Applied Geochemistry* 21 (4), 614–631.
- Pan, L., Oldenburg, C.M., Wu, Y.S., Pruess, K., 2009. Wellbore flow model for carbon dioxide and brine. *Energy Procedia* 1 (1), 71–78.
- Parkhurst, D.L., Appelo, C.A.J., 1999. *User's Guide to PHREEQC (version 2)—A Computer Program for Speciation, Batch-reaction, One-dimensional Transport, and Inverse Geochemical Calculations*. US Geological Survey Water Resources Investigation Report 99-4259, 312 pp.
- Pettyjohn, W.A., 1982. Cause and effect of cyclic changes in ground-water quality. *Ground Water Monitoring and Remediation* 2, 43–49.
- Piper, A.M., 1944. A graphic procedure in geochemical interpretation of water analyses. *Transactions American Geophysical Union* 25, 914–923.
- Plummer, L.N., Back, W., 1980. The mass balance approach; application to interpreting the chemical evolution of hydrologic systems. *American Journal Science* 280 (2), 130–142.
- Plummer, L.N., Busby, J.F., Lee, R.W., Hanshaw, B.B., 1990. Geochemical modeling of the Madison aquifer in parts of Montana, Wyoming, and South Dakota. *Water Resources Research* 26 (9), 1981–2014.
- Raines, M.A., Dewers, T.A., 1997. Dedolomitization as driving mechanism for karst generation in Permian Blaine Formation, Southwestern Oklahoma, USA. *Carbonates and Evaporites* 12, 24–31.
- Richter, B.C., Kreidler, C.W., 1986. *Geochemistry of Salt-Spring and Shallow Sub-surface Brines in the Rolling Plains of Texas and Southwestern Oklahoma*. The University of Texas at Austin, Bureau of Economic Geology Report of Investigations No. 155, 47 pp.
- Richter, B.C., Dutton, A.R., Kreidler, C.W., 1990. Identification of Sources and Mechanisms of Salt-Water Pollution Affecting Ground-Water Quality: A Case Study. The University of Texas at Austin, West Texas, Bureau of Economic Geology Report of Investigations No. 191, 43 pp.
- Saunders, J.A., Toran, L.E., 1994. Evidence for dedolomitization and mixing in Palaeozoic carbonates near Oak Ridge, Tennessee. *Ground Water* 32, 207–214.
- Simpkins, W.W., Fogg, G.E., 1982. Preliminary modeling of groundwater flow near salt-dissolution zones, Texas Panhandle. In: Gustavson, T.C. et al. (Eds.), *Geology and Geohydrology of the Palo Duro Basin, Texas*. The University of Texas at Austin, Bureau of Economic Geology Geological Circular 82-7, pp. 130–137.
- Smyth, R.C., Hovorka, S.D., Lu, J., Romanak, K.D., Partin, J.W., Wong, C., Yang, C., 2009. Assessing risk to fresh water resources from long term CO<sub>2</sub> injection—laboratory and field studies. *Energy Procedia* 1, 1957–1964.
- Stevens, P.R., 1974. *Geohydrology of the Upper Brazos River Basin between Lubbock and Possum Kingdom Reservoir, Texas, with Special Reference to Discharge of Brine from Springs and Seeps*. Austin, Texas, US Geological Survey, Water Resources Division, Open-File Report.
- Stotler, R.L., Frappe, S.K., El Mugammar, H.T., Johnston, C., Judd-Henrey, I., Harvey, F.E., Drimmie, R., Jones, J.P., 2011. Geochemical heterogeneity in a small, stratigraphically complex moraine aquifer system (Ontario, Canada): interpretation of flow and recharge using multiple geochemical parameters. *Hydrogeology Journal* 19 (1), 101–115.
- US EPA, 1993. Determination of inorganic anions by ion chromatography spectrometry. EPA Method 300.0 (revision 2.1), 28 pp.
- US EPA, 1994. Determination of trace elements in waters and wastes by inductively coupled plasma – mass spectrometry. EPA Method 200.8 (revision 5.4), 57 pp.
- US EPA, 1999. Total organic carbon in water. EPA Method 415.1, 3 pp.
- US EPA, 2001. Trace elements in water, solids, and biosolids by inductively coupled plasma-atomic emission spectrometry. EPA Method 200.7 (revision 5.0), 68 pp.
- Wang, S., Jaffe, P.R., 2004. Dissolution of a mineral phase in potable aquifers due to CO<sub>2</sub> releases from deep formations: effect of dissolution kinetics. *Energy Conversion and Management* 45 (18–19), 2833–2848.
- Wilkin, R.T., DiGiulio, D.C., 2010. Geochemical impacts to groundwater from geologic carbon sequestration: controls on pH and inorganic carbon concentrations from reaction path and kinetic modeling. *Environmental Science and Technology* 44, 4821–4827.
- Yang, C., Romanak, K.D., Smyth, R.W., Nicot, J.-P., Hovorka, S.D., Scanlon, B. Water-rock-CO<sub>2</sub> batch experiments and numerical modeling: implication for potential impacts of geological CO<sub>2</sub> sequestration on potable groundwater resources. *Environmental Earth Science*, under revision.
- Zehe, S., Becker, F., Heggemann, H., 2000. Dedolomitization by meteoric fluids: the Korbach fissure of the Hessian Zechstein basin, Germany. *Journal of Geochemical Exploration* 69–70, 173–176.
- Zhang, Y., Oldenburg, C.M., Finsterle, S., Jordan, P., Zhang, K., 2009. Probability estimation of CO<sub>2</sub> leakage through faults at geologic carbon sequestration sites. *Energy Procedia* 1 (1), 41–46.
- Zheng, L., Apps, J.A., Zhang, Y., Xu, T., Birkholzer, J.T., 2009. Reactive transport simulations to study groundwater quality changes in response to CO<sub>2</sub> leakage from deep geological storage. *Energy Procedia* 1, 1887–1894.